ISSN : 0974 - 7486 Volume 13 Issue 7

Materials Science

An Indian Journal

Full Paper

MSAIJ, 13(7), 2015 [226-236]

On the microstructural and mechanical characteristics of friction stir spot welded aa1050-o aluminum alloys

R.M.Afify*, T.S.Mahmoud, S.M.Abd-Rabbo, T.A.Khalifa

Mechanical Engineering Department, ShoubraFaculty of Engineering, Benha University, (EGYPT)

E-mail: Remasm7md@yahoo.com; tamer.abdelMagid@feng.bu.edu.eg; saberabdrabbo@yahoo.com; Tkhalifa50@yahoo.com

ABSTRACT

In the present investigation, the effect of friction stir spot welding (FSSW) parameters, typically, the tool rotation speed and dwell time on the microstructural and mechanical characteristics offriction stir spot welds aluminum alloy AA1050-O was investigated. The results revealed that the width of the completely metallurgical-bonded region (CMBR) increases with the increasing tool rotational speed and/or the dwell time up to certain levels. Increasing the tool rotational speed and/or the dwell time above these levels reduces the width of CMBR. Increasing the CMBR width increases the tensile-shear strength of the friction stir joint. The maximum tensile-shear force found in the present study was exhibited by the weld that has the CMBR width. The peak temperature measured during FSSW increases with increasing tool rotational speed and/or the dwell time. The maximum peak temperature observed was about 562 °C at 1600 rpm and 14 s.

KEYWORDS

Aluminum alloys;
Friction stir spot welding;
Mechanical properties;
Microstructure.

INTRODUCTION

The production of high quality aluminum joints using resistance spot welding (RSW) is a challenging task[1]. Consequently, aluminum sheet metal structures are often fabricated by riveting. Friction stir spot welding (FSSW)is a potentialalternative to riveting developed on the basis of Friction Stir Welding (FSW)[2]. In FSSW welds are produced using a non-consumable tool, consisting of a pin and a shoulder. The tool is rotated at a constant speed throughout the process. The sheet materials that are to be joined are placed one over another in lap configuration and are tightly clamped to an anvil. The rotating tool is gradually plunged into the sheets until the shoulder comes in contact with the upper sheet surface. Typically, the pin length is so chosen that it sufficiently penetrates into the lower sheet. Heat generated by friction softens the material being welded. The softened material is stirred resulting in intimate mixing of the upper and lower sheet materials. After a certain dwell time, the tool is withdrawn (no tool translation is involved). The result is a spot weld produced in the solid state between the upper and lower sheets with a central hole (pin hole).

Several investigators reported[3-6] that the effect of the FSSW process parameters on the mechanical characteristics of aluminum lap joints is diverse

which may be attributed to several reasons such as the nature of the welded alloys, variation of welding parameters, variation of sheet thickness, and tool design. In order to achieve a weld with sound joint integrity, a good understanding of the factors influencing the success of producing the welds is required. The frictional heat generated during the FSSW process softens the material and produces plastic flow that effectively stirs the materials of the sheets and fuses them together to create a weld[7]. It is thus essentially that the temperature during the FSSW process is monitored. Too little or too much heat generation will result in weak welds. Hence, it is very important to have an insight into the welding temperature[8-10]. The temperature generation is mainly a function of the tool rotational speed, dwell time and the interfacial pressure. The heat flow through the material is also dependent on the friction coefficient of the welding material and geometrical aspects of the rotating FSSW tool[7,11].

It is the aim of the present work is to investigate the effect of the FSSW process parameters, typically, the tool rotational speed and dwell time on the microstructural and mechanical characteristics of annealed AA1050-O aluminum alloy sheets joined by FSSW. Moreover, the effect of the aforementioned parameters on the temperature developed during FSSW was determined using thermal imaging camera.

EXPERIMENTAL PROCEDURES

In the present investigation, commercially pure aluminum AA1050-Oaluminum sheets having thickness of 4.3 mm were joined using FSSW. The AA1050 alloy has a nominal chemical compositions (in wt.-%): 0.0316% Cr, 0.0274% Ni, 0.009% Zn, 0.005% Mg, 0.002% Mn, 0.001% Cu, 0.343% Fe, 0.0543% Si, 0.0620% Ti, 99.4647% Al. The FSSW of AA1050-O aluminum alloy was performed using hardened K110 steel tool with a nominal chemical composition (in wt.-%): 0.165% C, 0.40% Mn, 11.30% Cr, 0.75% V, 0.75% Mo, 0.3% Si, and 86.335% Fe. The tool has a tapered pin and concave shoulder as shown in Figure 1. Such tool design provides a more refined Al microstructure and a stronger weld as opposed to a cylindrical design[17]. Additionally, a conical design was found to minimize the presence of a hook defect[18]. FSSW was conducted on AA1050-O Al sheets using a vertical milling machine with ûve different tool rotational speeds, typically, 630, 800, 1000, 1250, and 1600 rpm; and ûve different tool holding (dwell) times, typically, 6, 8, 10, 12, and 14 seconds. In all experiments, the toolpenetration depth and the tool plunger rate were held constantat 0.5 mm and[1] mm/min, respectively. Before welding, thesheets were cleaned with acetone to remove the oil and dirtimpurities from the surface.

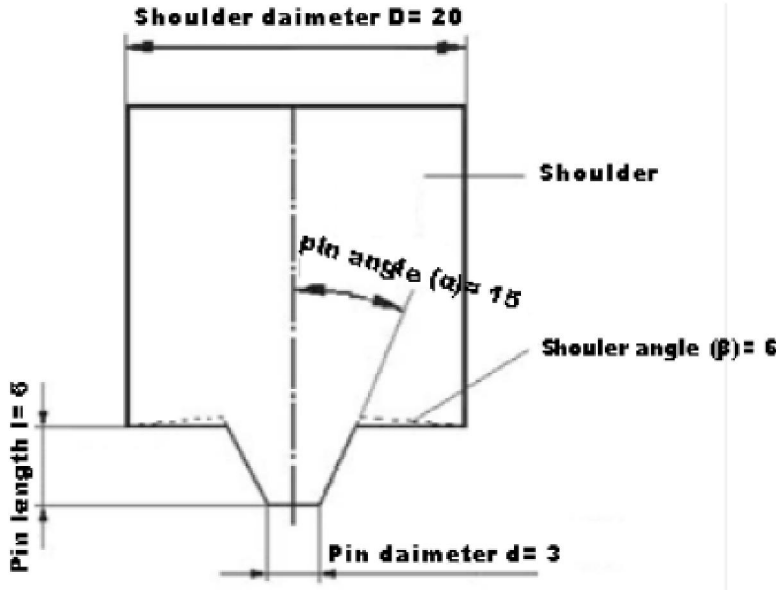

Figure 1 : A schematic illustration of FSSW tool (dimension in mm)

Full Paper

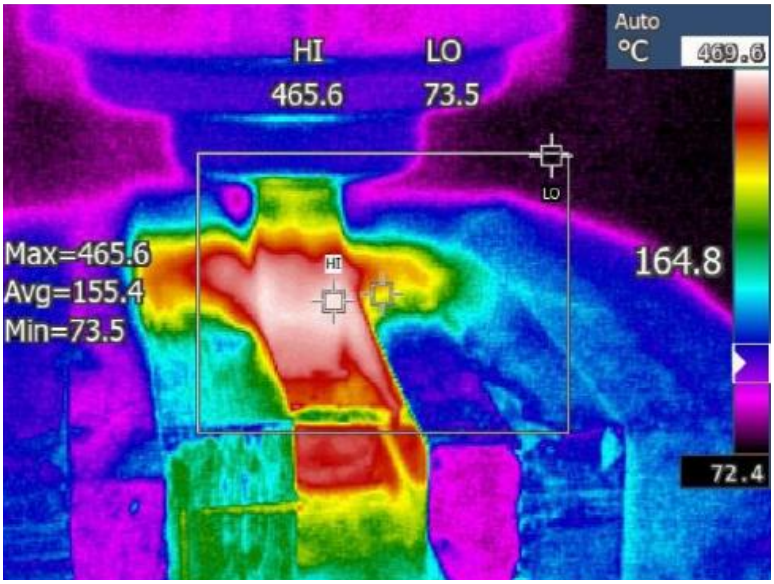

Figure 2 : A photograph illustrates the measurement of the temperature using thermal image camera

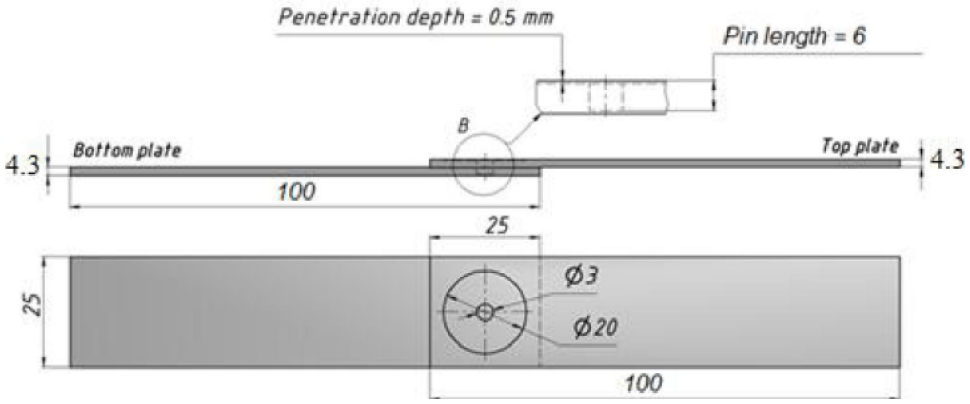

Figure 3 : A schematic illustration of the tensile-shear test specimen (Dimensions in mm)

The temperature distribution on the surface of AA1050-O Al sheets during FSSW were measured using *Fluke* Ti200 thermal imaging camera having a temperature measurement range from -20 °C to 650 °C. Thermal images were analyzed using *SmartView* imaging analysis and reporting software. Several recordings of the FSSW process were made for different tool rotational speeds and dwell times. In order to eliminate the reflected temperature from the field of view, objects such as anvil were coated by a commercial grade foot powder. The emissivity value set on camera was 0.25. Such a value was decided based on preliminary experiments. The view of sample image from the camera recorded during FSSW process is presented on the Figure 2.

The macro- and microstructural characteristics of FSSW AA1050-O sheets were investigated using optical microscope. The FSSW specimen was prepared according to the standard procedures for specimen preparation including grinding, polishing, and etching. Macroetching was carried out using a chemical solution, which consists of 100 mL H_2O, 50 mL HNO_3, 20 mL HF, and 30 mL HCl for 1-10 min at ambient temperature. Microetching was carried out using a chemical solution (0.5 mL HF 40% + 100 mL H_2O) for 5-120 s at an ambient temperature. Tensile-shear tests were conducted to evaluate the strength of FSSW joints. Lap-shear specimens were made using two 25 mm×100 mm coupons with 4 mm thickness and a 25 mm × 25 mm overlap area, at which the FSSW was performed at its center (see Figure 3). Tensile-shear tests were carried out at ambient temperature using a universal testing machine with a constant crosshead speed of 1 mm/min.

Vickers microhardness profile was measured on the traverse section along a plane 1 mm above the interface of the two overlapped sheets using an indenting load of 200 g and a loading time of 10 s. The fracture surfaces of the failed tensile specimens were examined using both digital camera and scanning electron microscope. The fractured surface area was calculated from the failed specimens using image analyzing techniques.

RESULTS AND DISCUSSION

Macro- and Microstructural Investigations

Figure 4 shows typical longitudinal cross-sections of FSSW joints processed with a constant tool rotational speed of 1000 rpm, and dwell times of 10 and 14 seconds. The indentationhole of the pin at the weld center is called a "keyhole". The light-grayareas near the keyhole periphery are stir zones (SZs). Aregion surrounded the SZ is a thermal mechanical affect zone(TMAZ), which has less heat input and plastic strain than thosein the SZ. Figure 5 shows higher magnification micrograph taken from the area close to the hook indicted by the arrow in Figure 4a. It is clear that different features are identiûed from the keyhole periphery along the interface of the two sheets; the complete metallurgical bond region (CMBR), partial metallurgical bond region (PMBR), and unbonded region (UR). The hook region is curved inwards towards the periphery of the pinhole in AA1050-O friction stir spot welds. This proûle of the hook was observed for most

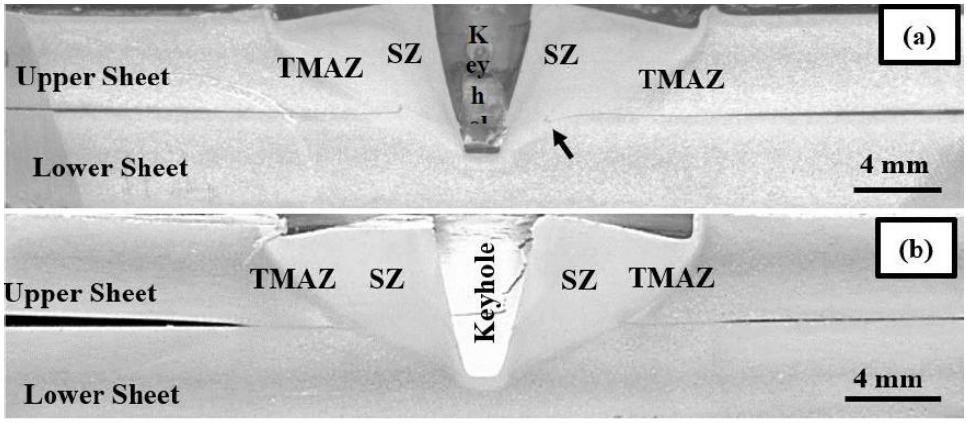

Figure 4 : Typical macrographs of the cross-sections of AA1050 friction stir spot welds made at constant tool rotational speed of 1000 rpm and various dwell times (a) 10 sec. and (b) 14 sec.

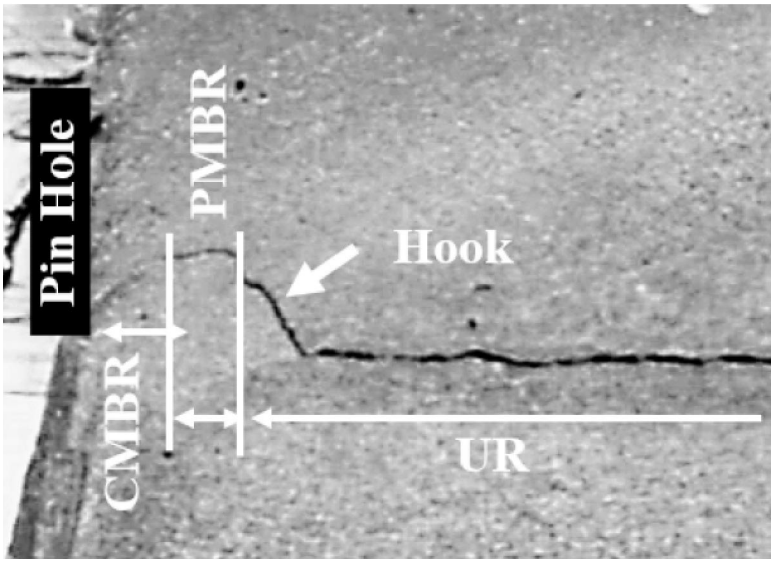

Figure 5 : Micrograph illustrating the different weld geometric features: the hook, unbounded region (UR), partially metallurgical-bonded region (PMBR), and CMBR

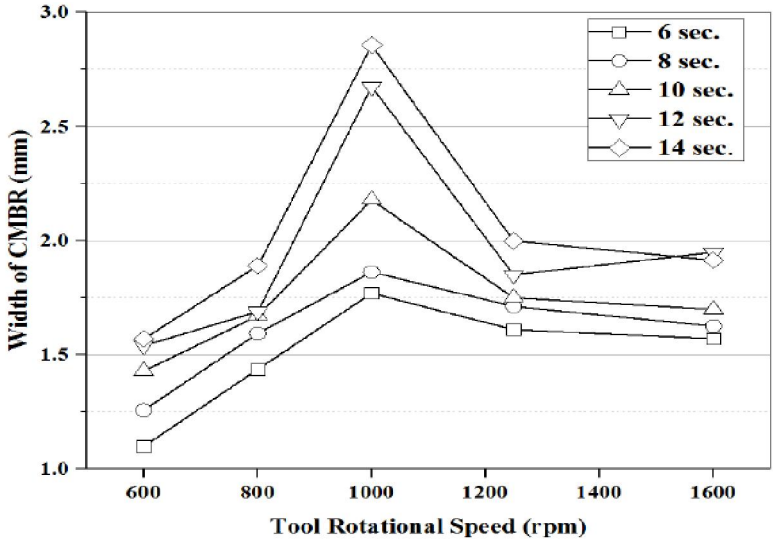

Figure 6 : Variation of the CMBR width with the tool rotational speedat various dwell times

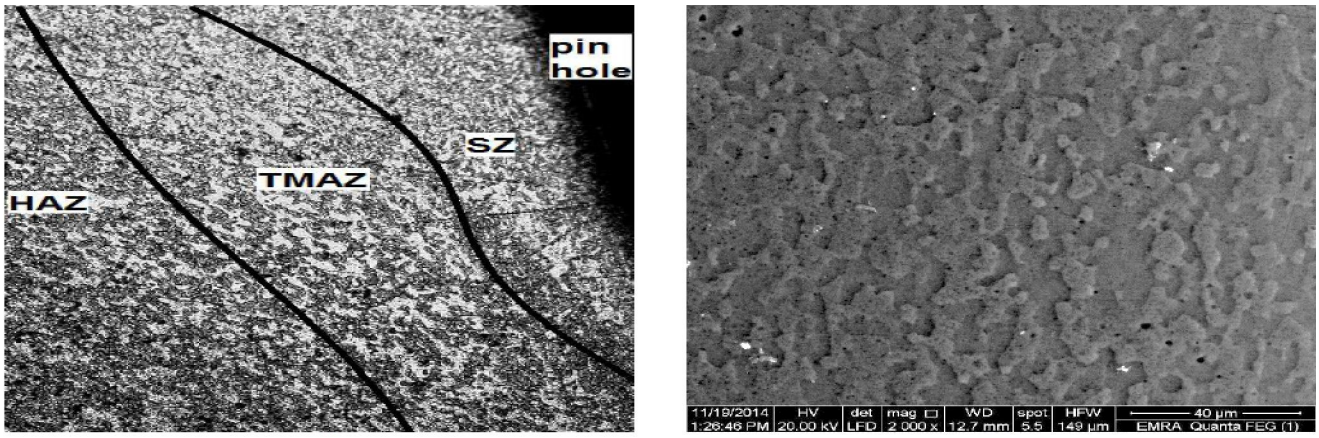

(a) **(b)**

Figure 7 : The microstructure of a cross-section of the weld made at welding condition of the rotational speed of 1250 rpm and dwell time of 12 s: (a) optical micrograph shows the SZ, TMAZ and HAZ regions, (b) High magnification SEM micrograph of the SZ region shown in (a)

welds. It has been reported that the formation of the hook is due to the upward bending of the initial joint interface after penetration of the tool in the lower sheet[12]. Since the material of the lower sheet is displaced upward, the hook is moved outward from the axis of the tool.

Figure 6 shows the variation of the CMBR width with tool rotational speed at several dwell times. The results revealed that, at constant dwell time, increasing the tool rotational speed up to a certain level increases the width of the CMBR. Increasing the tool rotational speed above this level reduces the width of the CMBR. For example, at constant dwell time of 6 seconds, increasing the tool rotational speed from 630 to 1000 rpm increases the width of the CMBR from 1.098 to 2.17915 mm. Further increase of the tool rotational speed higher than 1000 rpm reduced slightly the width of the CMBR. It has been noticed also that, at tool rotational speeds lower than 1200 rpm (i.e., 630,800 and 1000 rpm), increasing the dwell time increases the width of the CMBR. For example, at tool rotational speed of 630 rpm, increasing the dwell time from 6 to 14 seconds increases the width of the CMBR from 1.098 to 1.769 mm. Upon further increasing of the dwell time, the width of the CMBR remains either constant or slightly reduced. For example, at a constant dwell time of 8 seconds, increasing the rotational speed from 1000 to 1600 rpm slightly reduces the width of the CMBR. The maximum width of the CMBR was

about 2.857 mm for welds made using tool rotational speed of1000 rpm and dwell time of 14 seconds.

The increase of the CMBR width with the increasing tool rotational speed and/or the dwell time may be attributed to the increase of the frictional heat generated and the extension of the stirred interfacial region. Very high tool rotational speed and/or excessively rotational tool speed may increase(s) the temperature at the stirring zone to reach a value slightly lower than the melting point of the alloy. This significantly reduces the viscosity of the metal and hence reduces the shearing effect during stirring. The effects of tool rotational speed and the dwell time on the bonding width were reported by many investigators[3,13]. For example, Lin et al.[13] reported that when dwell time increased within a certain range, bonding width increased and then remained almost constant with further increase of dwell time. Such results are in agreement with those observed in the present study.

Figure 7 shows sample microstructure of the cross-section of a friction stir spot weld made at tool rotational speed and dwell time of 1250 rpm and 12 seconds, respectively. The stir zone (SZ), the thermo-mechanically affected zone (TMAZ) and Heat-affected zone (HAZ) are clearly seen in Figure 7a. Immediately beside the pinhole (keyhole) periphery the stir zonemicrostructure is comprised of very ûne α-Al grains. Such grains could not be observed using optical microscopy. Figure 7b shows higher magnification SEM micrograph of the SZ shown in Figure 7a. Figure 8 shows high magnification SEM micrograph of friction stir spot welds shown in Figure 5. The oxide film particles are clearly shown in the figure. It is suggested that the oxide particulates were formed due to the covering of oxide layers onto the Al surface. The oxide was either dispersed into fine particles or just extruded without significant dispersal. At lower tool rotation rates, the oxide layer at the faying surface is dispersed and shows a zigzag feature (indicated by the black arrow). Some discontinuous oxide debris (indicated by the white arrow) were identified at the boundary between the stir zone and TMAZ.

Peak temperature measurements during FSSW of AA1050-O Al Alloy

The variation of the peak temperature with tool rotational speed at several dwell times is illustrated in Figure 9. The peak temperature was measured at the shoulder/sheet contact surface during welding. It was found that both the tool rotational speed and dwell time aûect the peak temperature during welding. The peak temperature increases with increasing dwell time and/or tool rotational speed. For example, at constant dwell time of 14 s, the temperature increased from 485 to 562 °C when increasing the rotational speed from 630 rpm to 1600 rpm. The maximum peak temperature observed was about 562

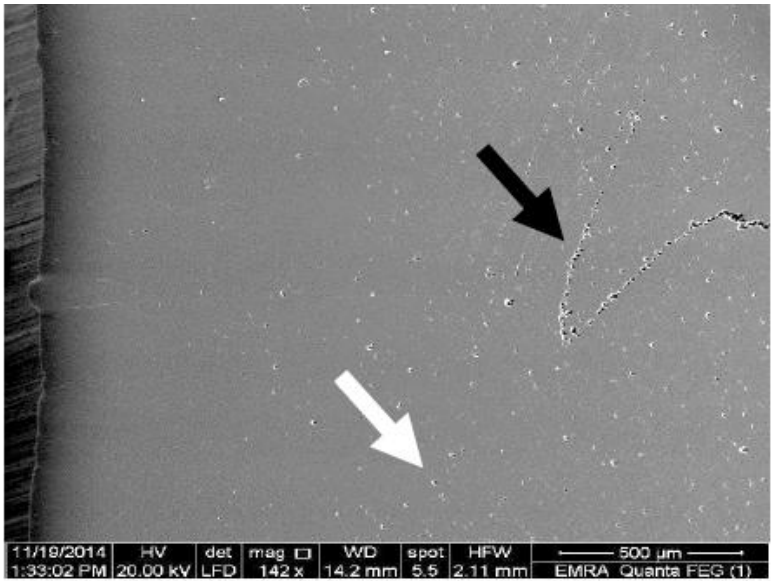

Figure 8 : SEM micrograph shows the oxide film distribution in AA1050-O friction stir spot welds

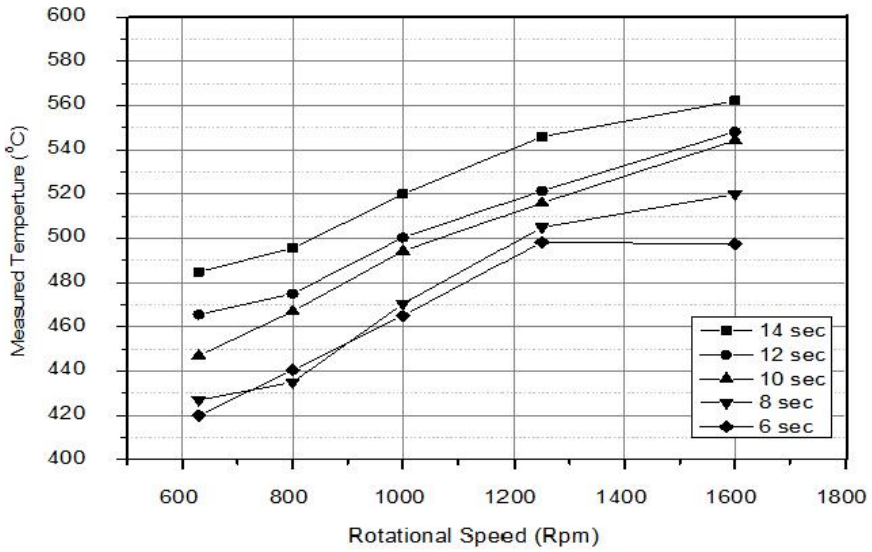

Figure 9 : The variation of the peak temperature with the tool rotational speed at several dwell times

°C at 1600 rpm and 14 s. The results observed in the present work was reported by many workers[13-16]. For example, *Toshiya et al.*[14] reported that during FSSW of pure aluminum sheets with 1 mm thickness, increasing the tool rotational speed from 500 to 1500 rpm, the temperature increased from 289 to 450 °C. Increasing tool rotational speed and/or the dwell time cause(s) the increase of the frictional heat generated during FSSW. It has been reported that very high tool rotational speed and/or excessively long dwell time may increase(s) the temperature at the stirring zone to reach a value slightly lower than the melting point of the alloy[3,10]. This significantly reduces the viscosity of the metal and hence reduces the shearing effect during stirring.

Microhardness tests

Figure 10 shows typical microhardness profiles of the welds at tool rotational speeds and dwell times of 4 and 8 s. In all the specimens, the microhardness profiles were found to be nearly symmetric with respect to the center of the pinhole. The results revealed that the welds have a higher microhardness in the stir zone than in the base material. The microhardness increases toward the direction of the pinhole. Increasing the tool rotational speed and/or the dwell time slightly reduce(s) the hardness of the weld. The influence of the dwell time on the hardness of the SZ was studied by *Lin et al.*[13]. They showed that the hardness distribution was somewhat scattered without noticeable trends. There was no obvious influence of process parameters on the hardness distribution. In another investigation carried out by *Zhang et al.*[4], they showed that the tool rotational speed and dwell time have little influence on the hardness of the welds.

Tensile-shear strength

The variation of the ultimate tensile-shear force with the tool rotational speed at different dwell times is represented in Figure 11. The results revealed that, at constant dwell time, increasing the tool rotational speed up to a certain level increases the tensile-shear force. Further increase in the tool rotational speed slightly reduces the tensile-shear force. For example, at constant dwell time of 10 s, increasing the tool rotational speed from 630 to 1000 rpm increases the tensile shear force from 2.2 to 3.57 kN. Further increase in the tool rotational speed to 1200 and 1600 rpm reduces the tensile shear force to about 2.5375 kN. Moreover, at constant tool rotational speed, increasing the dwell time increases the tensile-shear force. However, in most cases, increasing the rotational speed above 1000 rpm did not significantly increase the tensile-shear force. A maximum tensile-shear force of 4.63 kN was exhibited by the weld made using tool rotational speed of 1000 rpm and a dwell time of 14. The above results suggest that the combination of the tool rotational speed and dwell time plays a predominant role in deter-

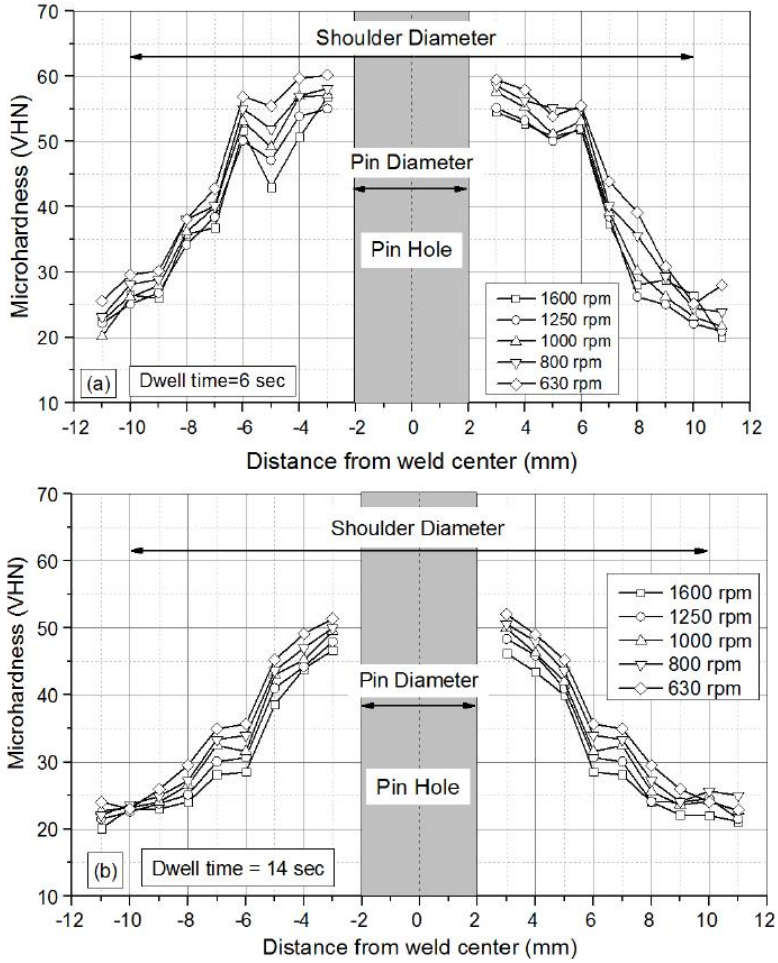

Figure 10 : Vickers microhardness distributions of welds at different tool rotational speeds and constant dwell time of (a) 6 sec. and (b) 14 sec.

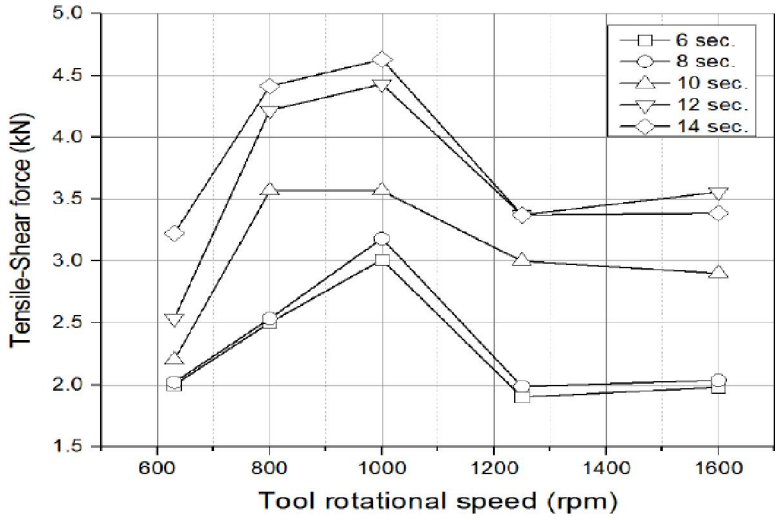

Figure 11 : Variation of the ultimate tensile-shear force with the tool rotational speed at several dwell times

mining the tensile-shear strength. Increasing the tool rotational speed and/or dwell time up to certain levels increase(s) the CMBR width. Upon increasing the tool rotational speed and dwell time above these levels, the CMBR width was found to be slightly reduced. Increasing the CMBR width increases the tensile-shear strength of the friction stir joint because of the increase of the contact area between upper

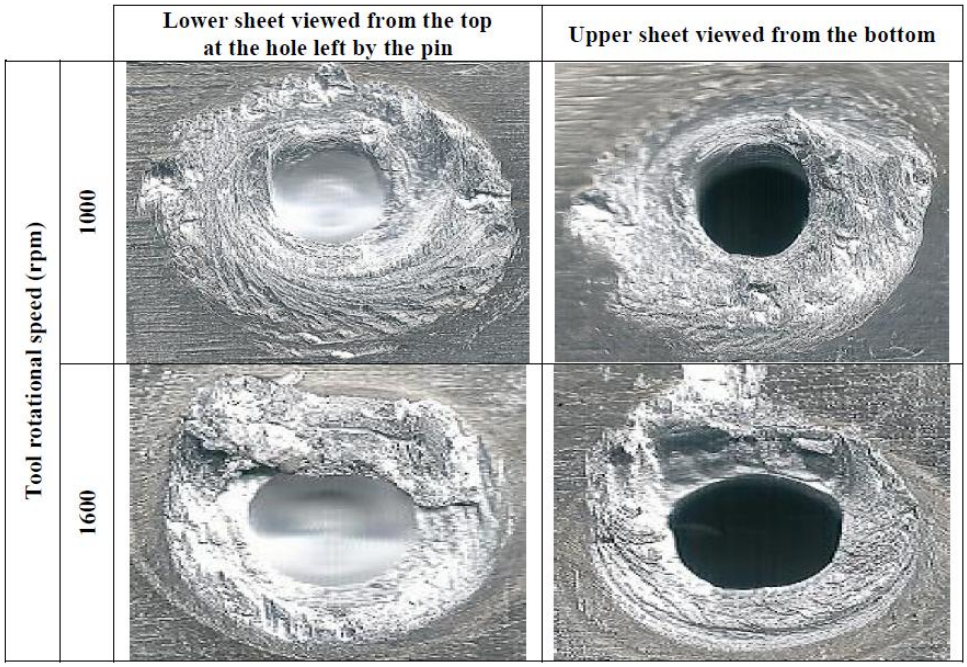

Figure 10 : Vickers microhardness distributions of welds at different tool rotational speeds and constant dwell time of (a) 6 sec. and (b) 14 sec.

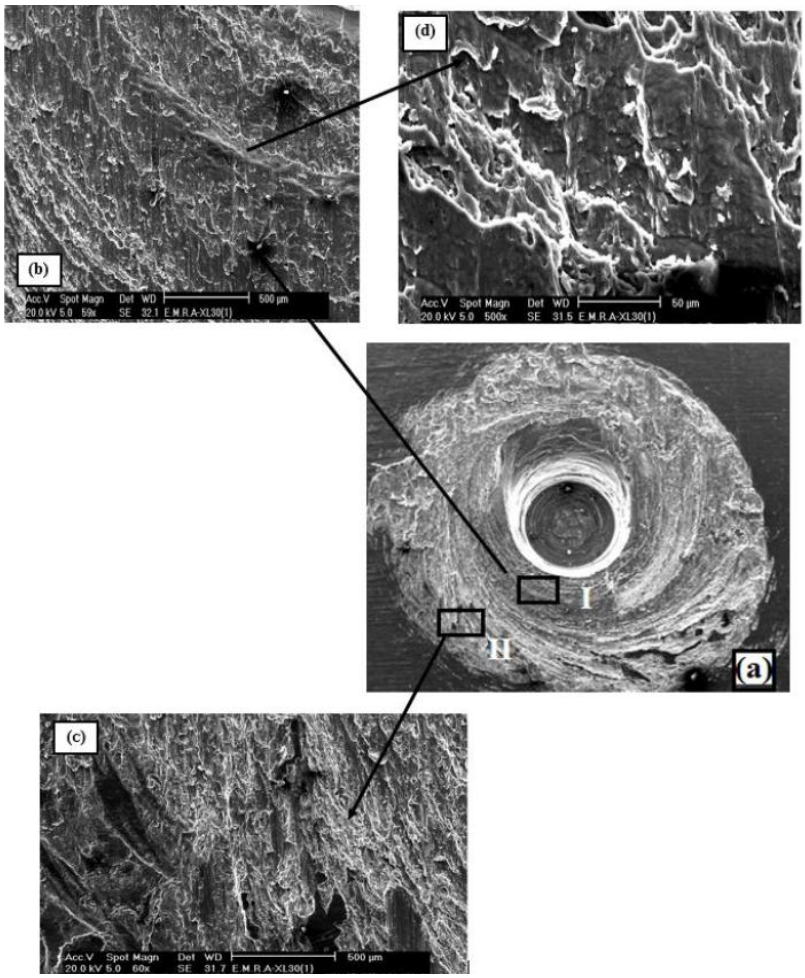

Figure 11 : Variation of the ultimate tensile-shear force with the tool rotational speed at several dwell times

and lower sheets. The maximum tensile-shear force found in the present study was exhibited by the weld that has the CMBR width.

Fracture morphology under tensile-shear loading

The failure modes in friction stir spot welds under tensile shear loading were investigated. Figure 12 shows photographs of typical failed specimens at the boundaries of the upper and lower sheets. Examination of the fractured surfaces revealed that the shear failure is the main failure mode which the boundaries between the upper and lower sheets are sheared-off. In addition, the circumferential failure mode (nugget pull-out) can be seen on the bottom sheet of the failed specimens.

Figure 13 shows SEM micrographs of the fracture surface of the lower sheet of tensile-shear sample welded under the conditions of tool rotational speed of 1000 rpm and dwell time of 10 s. Examination of the fracture surfaces revealed that different failure modes had occurred during the tensile-shear tests. According to the SEM micrographs of region II presented in Figure 13(c), elongated dimples near the outer circumference of the welded region are present indicating the occurrence of shear fracture in region II. Figure 13(b) and (d) show SEM micrographs of region I in the position near the inner circumference of the welded region. Numerous tear ridges and small shallow dimples were observed, which suggests the occurrence of mixed-type rupture containing dimple fracture and quasi-cleavage fracture. Observations of the fractured tensile-shear specimens suggest that all cracks initiate at the hook tip. The cracks then propagate along the partial bonding interface and continue across the bonding interface along the circumferential direction of the weld. Finally, the fracture occurs because of the decreasing load carrying area.

CONCLUSION

Based on the results presented, the following conclusionscan be drawn:

Increasing the tool rotational speed and/or dwell time up to a certain level increase(s) the width of the CMBR. Increasing the tool rotational speed and/or the dwell time above this level reduces the width of the CMBR. The maximum width of the CMBR was about 2.857 mm for welds made using tool rotational speed of 1000 rpm and dwell time of 14 seconds.

The peak temperature increases with increasing dwell time and/or tool rotational speed. The maximum peak temperature observed was about 562 ^{o}C at 1600 rpm and 14 s.

Increasing the tool rotational speed and/or the dwell time up to a certain level improve(s) the tensile-shear strengthof the welds. Increasing the tool rotational speed and the dwell time higher than these levels slightlyreduce the tensile-shear strength. Samples friction stir spot welded under the conditions of tool rotational speedof 1000 rpm and dwell time of 14 s exhibited the maximum tensile-shear force of 4.63 kN. The maximum tensile-shear force found in the present study was exhibited by the weld that has the CMBR width.

The SZs exhibited higher microhardness than that of the base material. Increasing the tool rotational speed and/or thedwell time reduce(s) slightly the microhardness at the SZ.

ACKNOWLEDGEMENTS

The authors are thankful to the Benha University – Shoubra Faculty of Engineering for providing financial support for carrying out this study.

REFERENCES

[1] H.Zhang, J.Senkara; "Resistance welding: Fundamentals and applications", Taylor &Francis, ISBN, **13**, 978-0-8493-2346-1 **(2006)**.

[2] R.S.Mishra, M.W.Mahoney; "Friction Stir Welding and Processing", ASM, **(2007)**.

[3] T.S.Mahmoud, T.A.Khalifa; "Microstructural and mechanical characteristics of aluminium alloy AA5754 friction stir spot welds", Journal of Materials Engineering and Performance, **23(3)**, 898-905 **(2014)**.

[4] Z.Zhang, X.Yang, J.Zhang, G.Zhou, X.Xu, B.Zou; "Effect of welding parameters on microstructure and mechanical properties of friction stir spot welded 5052 aluminum alloy", Materials & Design, **32**, 4461–4470 **(2011)**.

Full Paper

[5] E.Salari, M.Jahazi, A.Khodabandeh, H.Ghasemi-Nanes; "Influence of tool geometry and rotational speed on mechanical properties and defectformation in friction stir lap welded 5456 aluminum alloy sheets", Materials & Design, **58**, 381–389 **(2014)**.

[6] Z.Shen, X.Yang, S.Yang, Z.Zhang, Y.Yin; "Microstructure and mechanical properties of friction spot welded 6061-T4 aluminum alloy", Materials & Design, **54**, 766–778 **(2014)**.

[7] Q.Yang, S.Mironov, Y.S.Sato, K.Okamoto; " Material flow during friction stir spot welding", Materials Science and Engineering A, **527(16–17)**, 4389–4398 **(2010)**.

[8] K.J.Dharmaraj, C.D.Cox, A.M.Strauss, G.E.Cook; "Ultrasonic thermometry for friction stir spot welding", Measurement, **49**, 226–235 **(2014)**.

[9] S.Mandal, J.Rice, A.A.Elmustafa; "Experimental and numerical investigation of the plunge stage in friction stir welding", journal of materials processing technology, **203**, 411–419 **(2008)**.

[10] M.Merzoug, M.Mazari, L.Berrahal, A.Imad; "Parametric studies of the process of friction spot stir welding of aluminium 6060-T5 alloys", Materials & Design, **31(6)**, 3023–3028 **(2010)**.

[11] W.Yuan, R.S.Mishra, B.Carlson, R.Verma, R.K.Mishra; "Material ûow and microstructural evolution during friction stir of AZ31 magnesium alloy spot welding", Materials Science and Engineering A, **543**, 200-209 **(2012)**.

[12] Y.H.Yin, N.Sun, T.H.North, S.S.Hu; "Hook Formation and mechanical properties in AZ31 friction stir spot welds", J.Material Processing Technology, **210(14)**, 2062–2070 **(2006)**.

[13] Yuan-Ching Lin, Ju-Jen Liu, Ben-Yuan Lin, Chun-Ming Lin, Hsien-Lung Tsai; "Effects of process parameters on strength of Mg alloy AZ61 friction stir spot welds", Materials and Design, **35**, 350–357 **(2012)**.

[14] Shibayanagi Toshiya, Mizushma, Yoshiawa Shyuhei; "friction stir spot welding of pure aluminum sheet in view of high temperature deformation",Transcations of JWRI, **40**, 1-5 **(2011)**.

[15] Adrian Gerlich, Peter Su,Motomichi Yamamoto, Tom H.North; "Effect of welding parameters on the strain rate andmicrostructure of friction stir spot welded 2024 aluminum alloy", Journal of Materials Science, **42**, 5589–5601 **(2007)**.

[16] N.Pathak,K.Bandyopadhyay, M.Sarangi, Sushanta Kumar Panda; "Microstructure and Mechanical Performance of Friction Stir Spot-Welded Aluminum-5754 Sheets" Journal of Materials Engineering and Performance, **22(1)**, 131-144 **(2013)**.

[17] H.Badarinarayan, Y.Shi, X.Li, Okamoto; "Effect of tool geometry on hook formation and static strength of friction stir spot welded aluminum 5754-O", International Journal of Machine Tools & Manufacture", **49**, 814–823 **(2009)**.

[18] Mustafa Kemal Bilici, Ahmet, IrfanYükler; "Inûuence of tool geometry and process parameters on macrostructure and static strength in friction stir spot welded polyethylene sheets", Materials and Design, **33**, 145–152 **(2012)**.